Analyst

Accepted Manuscript

ROYAL SOCIETY OF CHEMISTRY

www.rsc.org/analyst

Table of contents entry

Highly stable and copper-responsive fluorescent silver nanoclusters were assembled on human ferritin with retained structures and functions of ferritin template as well as fused binding proteins.

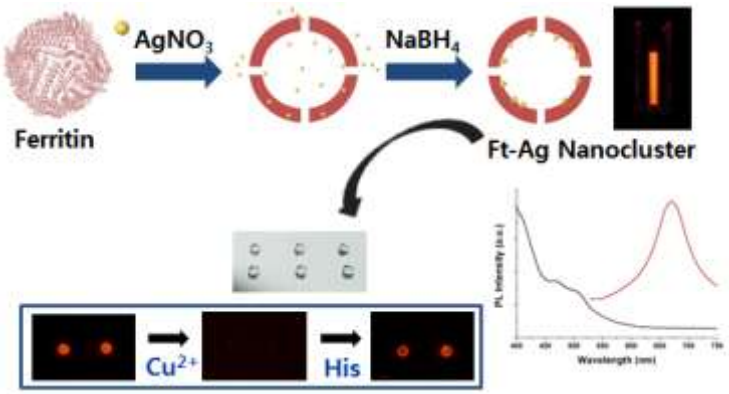

A Facile Synthesis of Fluorescent Silver Nanoclusters with Human Ferritin as a Synthetic and Interfacing Ligand

In Hwan Lee[a], Byungjun Ahn[a], Jeong Min Lee[a], Chang Soo Lee[b], and Yongwon Jung[a]*

Table of contents entry

Highly stable and copper-responsive fluorescent silver nanoclusters were assembled on human ferritin with retained structures and functions of ferritin template as well as fused binding proteins.

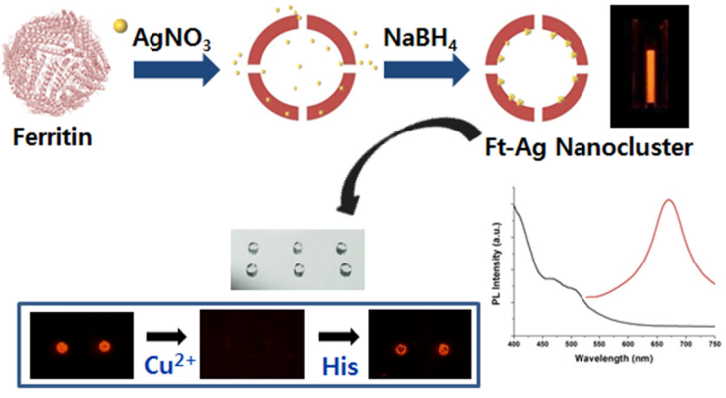

Abstract

Water-soluble fluorescent silver nanoclusters (NCs) formed on biomolecule ligands have been extensively studied due to their great potential as new biocompatible fluorescent materials for biosensors. As synthetic ligands, proteins in particular can provide unique structures and functions to assembled fluorescent silver clusters. A key challenge, however, is to develop proper protein ligands and synthetic approaches for cluster formation, especially in native aqueous solutions to fully preserve valuable properties of protein templates. Here we report a human ferritin-templated synthesis of fluorescent silver NCs under a neutral aqueous buffer condition. The unique metal binding property of ferritin and optimized silver ion reduction allowed us to produce highly stable fluorescent silver NCs that are steadily assembled in cage-like ferritin proteins. The fluorescent clusters were also successfully assembled on genetically engineered ferritin with antibody-binding protein G. The resulting protein G-ferritin-silver NC complex fully retained the ferritin structure as well as the antibody binding ability. The present silver nanoclusters on ferritin (Ft-Ag NCs) also showed highly specific Cu^{2+}-induced fluorescence quenching. By exploiting the large but stable nature of ferritin, we fabricated a highly robust and porous hydrogel sensor system for rapid Cu^{2+} detection, where Ft-Ag NCs were stably encapsulated in surface-bound hydrogels with large pore sizes. Our Ft-Ag NCs that are formed under native aqueous condition will have great potential as new fluorescent material with high structural and functional diversities of ferritin.

Introduction

Noble metal nanoclusters (NCs), such as gold and silver clusters, with intrinsic fluorescence properties have received great attention due to their small size, superior photo-stability, and low toxicity, which are highly beneficial features for biological imaging and sensing.[1-3] Multiple synthetic strategies have been developed to prepare fluorescent and water-soluble novel metal NCs.[4, 5] Compared with gold NCs, the synthesis of stable silver NCs has been highly challenging due to their higher tendency to aggregate in aqueous solutions. Strong capping reagents or pre-formed template ligands were needed to fabricate and stabilize silver NCs in water.[6, 7] In particular, DNA has been widely used to construct water-soluble and fluorescent silver NCs.[8-11] These DNA-templated silver clusters have shown strong environmental sensitivities, and thereby have been utilized in the detection of various molecules, especially DNA and RNA targets.[12, 13]

Proteins can be also powerful template ligands for the synthesis of fluorescent metal clusters with their unlimited structural and functional diversities. Various functions can be added to protein templates to generate new functional fluorescent probes. The complexity of proteins, however, made it difficult to design protein templates for efficient cluster formation. In contrast to numerous examples of DNA-templated synthesis, only few studies have demonstrated the use of full proteins for silver NC formation.[14-18] Several proteins including serum albumin proteins[14-16], lysozyme[17], and chymotrypsin[18] were employed to direct the creation of fluorescent silver NCs. These approaches, however, required protein templates to be in non-native conditions, where proteins were fully denatured[14] or in highly basic solutions[15-17]. To fully retain structural accuracy and functionalities of proteins as synthetic templates for silver NCs, strategies for cluster formation under native conditions are highly desired.

Ferritin is one of the most widely used protein scaffolds in the field of nano-assembly with its unique cage structure and rich functions.[19] The protein is composed of 24 protein subunits of two types, the heavy and light chains, that assemble to form a spherical shell with a cavity of about a 8 nm diameter.[20] This cage protein, which is involved in the physiological iron storage, can also bind various metal ions in its cavity, and this metal binding property has been extensively used to synthesize a number of different metal nanoparticles (including noble metal nano-structures) in the protein shell.[19, 21, 22] Previously, gold clusters were assembled in horse spleen ferritin, which can be targeted to mouse kidney.[23] Silver nanoparticles were also formed inside the cages of ferritin proteins from different sources.[24-26] We therefore envisioned that careful control of silver ion deposition in ferritin may allow the construction of fluorescent silver NCs, stably assembled in a native protein.

Here we report a facile synthesis of fluorescent silver NCs in a mild aqueous buffer solution by employing recombinant human ferritin as a stabilizing and also interfacing ligand (Fig. 1a). The degree of silver ion reduction on a heavy chain ferritin cage was thoroughly varied in buffered water, producing silver nanostructures with various sizes from clusters to particles. Fluorescent silver NCs were obtained only with a narrow range of ratios between ferritin and silver ions. These ferritin-templated fluorescent silver NCs (Ft-Ag NCs) were stable in physiological buffer conditions, retaining their fluorescence as well as protein structures. The clusters were also stably formed on engineered ferritin, fused with antibody-binding protein G, of which binding ability was maintained after silver NC formation. In addition, Ft-Ag NCs showed Cu^{2+} specific fluorescence quenching as previously reported with other silver NCs.[27-30] We demonstrated encapsulation of the Ft-Ag NC-based sensor to a surface hydrogel system (Fig. 1b). Unique properties of both ferritin (large but robust) and silver NCs (stably fluorescent) provided a highly stable (even in dry or extreme pH conditions) and porous hydrogel sensor system for rapid Cu^{2+} detection.

Results and discussion

Synthesis of silver nanoclusters on human ferritin

Silver nanoclusters (NCs) on biomolecular templates are generally prepared by initial silver ion binding to the pre-formed template and subsequent reduction of silver ions to form clusters.[6] Stabilizing templates and reduction conditions must be carefully selected to control the growth of silver clusters and to prevent the formation of larger particles or precipitation. Previously, small silver nanoparticles (~2 nm) were synthesized by templated reduction of silver ions on an archaeal ferritin, but massive precipitation was observed on human ferritin templates.[25] Human ferritins are known to have a high number of potential metal binding sites, which may lead to un-controllable growth of silver particles. On the other hand, we also hypothesized that abundant metal binding sites of human ferritin can be advantageous for silver NC formation by favoring more scattered metal nucleation. Silver ion reduction, however, must be precisely controlled (likely slowed) to prevent association of small clusters.

To prepared silver NCs, silver ions ($AgNO_3$) and reducing agent ($NaBH_4$) were sequentially added to heavy chain human ferritin in 20 mM HEPES pH 7.2. Chloride ions in reaction solutions, however, caused irregular aggregation of various silver nanostructures, regardless of buffer systems (Fig. S1 in ESI). Therefore, ferritin proteins were extensively dialyzed against the reaction buffer to completely remove residual chloride ions, and buffer solutions for silver cluster formation were also prepared free from chloride ions. The molar ratio between human ferritin and $AgNO_3$ was varied from 1:100 to 1:2000 to optimize the growth of silver NCs. Here relatively low concentration of protein (0.2 μM, 0.1 mg/mL)[14, 15] and consequently low levels of Ag^+ were used to ensure nucleation of small silver clusters. Added $NaBH_4$ concentration was also fixed at 50 μM (protein:$NaBH_4$ = 1:250), rather than equivalently increased with Ag^+. Hence, silver ion reduction on ferritin was incrementally varied by controlling Ag^+ concentration under diluted protein and reductant condition.

As the protein/$AgNO_3$ ratio increased, the growth of silver nanostructure was clearly observed (Fig. 2). Silver nanoparticles larger than 2 nm were produced with ferritin/ $AgNO_3$ ratios over 1:700 (Fig. 2a and Fig. S2 in ESI). TEM images indicate that the nanoparticles were formed with narrow size distributions, and major size populations were increased from ~2 nm to ~8 nm (Fig. S2 in ESI). Maximum particle sizes were below 9 nm, possibly due to the size of the ferritin cavity (~8 nm).[20] Silver nanoparticles also showed their unique and size-dependent optical properties such as increased absorption peaks at 450 nm and brown colors (Figs 2b, 2c). The fabricated silver NCs on ferritin templates were also analyzed by agarose gel electrophoresis (Fig. S3 in ESI). A narrow migration band of ferritin was maintained even with various levels of silver ion reduction, although the migration was slightly (but gradually) slowed as Ag^+ concentration increased. Silver nanoparticles were also co-migrated with ferritin proteins, indicating stable assembly of silver nanostructures with ferritin in the hydrophilic gel condition. These data suggest several beneficial roles of ferritin for silver nanostructure formation. The active metal uptake property of human ferritin with its abundant metal binding sites may promote scattered but precise control of silver deposition even under diluted protein and metal concentrations without the need of denaturing proteins to expose metal binding sites. In addition, an isolated reaction space of ferritin might contribute to homogeneous growth of silver nanostructures as well as protection of assembled structures from aqueous buffer solution.

Characterization of fluorescent silver nanoclusters on human ferritin

Fluorescent properties of silver NCs on ferritin (Ft-Ag NCs) in aqueous buffer solutions were examined under various excitation lights. The maximal fluorescent signal (at 695 nm) was emitted from the reaction solution with the protein/$AgNO_3$ ratio 1:500 under a 470 nm light (Fig. 2d). The signal was increased with added Ag^+ (from 1:100 to 1:500) but

quickly disappeared as silver nanoparticles formed, hinting the formation of fluorescent silver NCs optimally at the protein/$AgNO_3$ ratio 1:500. Even a slight increase of Ag^+ (the protein/$AgNO_3$ ratio 1:700) caused nanoparticle formation and vastly diminished fluorescent signals. A narrow range of Ag^+ concentration under diluted protein and reductant condition was required for fluorescent silver NC formation on human ferritin template. Although silver NCs were not directly observed by a TEM analysis (Fig. 2a), the absorbance and fluorescence emission profiles were similar to those of previously reported silver NCs synthesized on various biomolecules (Fig. 3a).[9, 14, 17, 18] The present Ft-Ag NCs showed a maximum fluorescence emission at 673 nm when excited at 465 nm and retained this fluorescence intensity even after one month at room temperature. A TEM-EDS (Energy-dispersive X-ray spectroscopy) analysis confirms the silver metals assembled with ferritin proteins (Fig. S4 in ESI). Several studies reported thiol-induced fluorescence quenching of fluorescent silver NCs synthesized on DNA templates.[31-33] Our Ft-Ag NCs were also fluorescently quenched by 1 h incubation with DTT (Fig. S5 in ESI). The quantum yield of Ft-Ag NCs was examined with rhodamine B in ethanol as the reference standard.[34] An estimated value was 1.74%, which is again close to the reported quantum yield of silver NCs synthesized on BSA (~1.2%).[14]

The mass difference between free ferritin and Ft-Ag NCs were examined with matrix-assisted laser desorption ionization time-of-flight (MALDI-TOF) mass spectroscopy to determine the compositions of silver NCs. Three mass peaks for monomer (21120 Da), dimer (42175 Da), and trimer (63268 Da) of human ferritin, which is originally a 24-meric cage protein, were observed (Fig. S6 in ESI). These peaks were clearly shifted by silver cluster formation, although the degrees of shifts were varied from monomer (201 Da), dimer (505 Da), to trimer (1186 Da). The mass shift on trimer corresponds to approximately 11 atoms of silver, which is close to previous red emitting fluorescent silver clusters (between 10 to 13 silver atoms).[35-37] Extensive disassembly of the ferritin cage down to even monomer

might result in cluster detachment from protein or cluster cleavage, leading to smaller and heterogeneous mass shifts. Previous studies on mass analyses of various fluorescent silver nanoclusters also reported a wide range of cluster sizes including small clusters (one to five atoms)[38, 39] and even no clear observation by mass spectroscopy[14, 17]. Although the exact size of silver clusters could not be determined in the present study, MALDI-TOF data supported the stable assembly of silver nanoclusters on ferritin.

Here chloride ions were detrimental for homogeneous synthesis of silver nanostructures on ferritin. Interestingly, however, after silver reduction, we were able to collect assembled Ft-Ag NCs by simple centrifugation with added 50 mM NaCl (Fig. S7 in ESI). The centrifuged pellets were easily resuspended in various aqueous buffers, and this process can be repeated without losing fluorescence intensities. This behavior of fluorescent Ft-Ag NCs enabled rapid purification and buffer exchanges of the clusters in a high yield. Here thereby water-soluble and fluorescent Ft-Ag NCs were consistently prepared and purified in less than 30 min. The TEM image of purified Ft-Ag NCs shows well-dispersed ferritin proteins without any irregular large protein aggregates (Fig. 3b), which is also supported by above gel migration data (Fig. S3 in ESI). In addition, resuspended Ft-Ag NCs fully entered a desalting gel-filtration column, again showing no protein aggregates (data not shown). Chloride ions may induce large, high-order, and reversible complex formation between silver NC-assembled ferritin proteins. However, more studies must follow to elucidate the mechanism of chloride-induced changes of Ft-Ag NCs.

We next investigated if our approach for silver NC formation in native condition would allow functionalization of fluorescent Ft-Ag NCs by simply fusing a functional protein to the ferritin template. Antibody-binding protein G was genetically fused to the N-terminus of ferritin. Resulting protein G-fused ferritin displays 24 protein G proteins on the ferritin cage surface. Fluorescent silver NCs were successfully formed on this protein G-ferritin

template under the same protein/$AgNO_3$ ratio (1:500). A TEM analysis indicated that protein G-ferritin with assembled silver NCs (PG-Ft-Ag NCs) maintained its cage structure with a slightly increased diameter, likely due to fused 24 protein G proteins (Fig. 3c). The gel migration pattern of protein G-covered Ft-Ag NCs was also similar to that of Ft-Ag NCs. Antibody binding ability of PG-Ft-Ag NCs was confirmed by both TEM and gel electrophoresis analyses (Fig. 3c). The cage structure of PG-Ft-Ag NCs was clearly enlarged by interaction with large antibodies (~15 nm), and gel migration was also visibly shifted by antibody binding. The data demonstrated that functionally engineered ferritin proteins can also be used as templates for fluorescent silver NC synthesis, while retaining structures and functions of the proteins. Protein G-covered Ft-Ag NCs can be utilized as valuable fluorescent immuno-labels with ability to bind and display antibodies with ideal orientations for subsequent antigen interactions.

Fluorescent silver nanoclusters on human ferritin for Cu(II)-specific biosensor

Most silver NCs formed on biomolecular templates have shown fluorescence quenching by divalent metal ions, especially Cu^{2+} and Hg^{2+}.[14, 27-29, 40] We investigated fluorescence responses of Ft-Ag NCs against an array of metal ions (Ca^{2+}, Cd^{2+}, Co^{2+}, Cr^{2+}, Cu^{2+}, Fe^{2+}, Hg^{2+}, Mg^{2+}, Mn^{2+}, Ni^{2+}, and Pb^{2+}). As shown in Fig. 4a, the fluorescence intensity of Ft-Ag NCs was significantly quenched only by Cu^{2+}. This copper-selective fluorescence quenching is commonly observed in DNA-templated silver NCs.[27-29, 31] Fluorescent silver NCs on denatured serum albumin proteins showed quenching responses to either Hg^{2+} [14] or Co^{2+} [15]. Copper concentration dependency of fluorescence quenching is subsequently evaluated by varying Cu^{2+} concentration from 10 nM to 1 mM. The fluorescence intensities were gradually decreased as copper concentration increases (Fig. 4c). The fluorescent intensity at 673 nm was plotted against Cu^{2+} concentration, and a linear dynamic range from

10 nM to 0.1 mM was obtained for Cu^{2+} detection (Fig. 4d). The dynamic range and estimated detection limit (~100 nM) are well-comparable to previously reported Cu^{2+} sensors using fluorescent silver NCs.[28, 29, 31]

Hydrogels are attractive surface coating materials for biosensors by offering low biofouling, high receptor densities, and controllable pore sizes for selective target diffusion. An aqueous environment of hydrogel is particularly beneficial for surface immobilization and storage of protein-based biosensors. A key challenge, however, is to optimally control the pore size to ensure rapid penetration of target molecules but prevent diffusion of encapsulated protein sensors. Typical protein sensors are thereby covalently linked to the hydrogel matrix on sensor surfaces. Our copper sensing silver NCs are, however, assembled on large but robust ferritin proteins, which can be entrapped in hydrogels with large pore sizes for rapid target approaches. Previously small fluorescent silver clusters were formed within peptide-based hydrogels.[38, 39] Here, we encapsulated Ft-Ag NCs in low density acrylamide hydrogels (4%) by simply spotting the solution mixtures, containing hydrogel precursor acrylamide and Ft-Ag NCs, on an acrylate-terminated glass surface. Transparent hydrogel spots were formed with clear fluorescence emissions from encapsulated Ft-Ag NCs (Fig. 5a).

Fluorescent Ft-Ag NCs in acrylamide hydrogels showed remarkable stability under several extreme conditions (Fig. 5a). Hydrogel chips were stored in hydrated as well as dried forms without losing fluorescent signals and gel shapes. In addition, fluorescent intensities were not affected by extreme pH conditions from 2 to 12. High molecular weight (~500 kDa) ferritin proteins with silver NCs were also stably embedded within hydrogels even after 1 h incubation in an aqueous solution, whereas smaller green fluorescence protein (GFP, 27 kDa) diffused out from the hydrogels (Fig. 5b). We finally investigated copper detection by using the hydrogel-encapsulated Ft-Ag NCs. The hydrogel sensor chip was directly dipped into a 0.1 mM Cu^{2+} solution. Fluorescent signals of soaked hydrogel spots were rapidly quenched

within 1 min (Fig. 5c). The low density (4% acrylamide) hydrogels likely allow the free movement of Cu^{2+} in and out of the hydrogel matrix. An amino acid histidine has been reported to form a stable complex with Cu^{2+} and therefore utilized for fluorescence recovery after Cu^{2+}-induced quenching of DNA-templated silver NCs.[30] Here histidine treatment also quickly induced fluorescence recovery of the Ft-Ag NCs (82% of the original fluorescence intensity) (Fig. 5c). Collectively we demonstrated that unique structural and functional properties of ferritin and assembled silver NCs enabled the construction of a highly stable and porous hydrogel sensor system for Cu^{2+}. In particular, surprisingly high stability of the protein-hydrogel Cu^{2+} sensor (even under dried or extreme pH conditions) will be highly beneficial for designing environmental copper detection systems, which often require prolonged sensor activities under extreme conditions.

Experimental

Materials. Silver nitrate ($AgNO_3$), Sodium borohydride ($NaBH_4$), 3-(Trichlorosilyl)propyl methacylate (TPM), 2-Hydroxy-2-methylpropiophenone, Rhodamine B, and human immunoglobulin G (hIgG) were purchased from Sigma. 20 mM HEPES (4-(2-hydroxyethyl)-1-piperazineethanesulfonic acid) buffer was prepared immediately before use by titrating to pH 7.2 with 1 M NaOH.

Preparation of recombinant ferritin proteins. Human heavy chain ferritin (Ft) and protein G-fused Ft (PG-Ft) were cloned in pET21a expression vector and expressed in *E. coli* (BL21(DE3), Novagen). Bacterial cultures containing related plasmids were grown overnight at 37 °C. The ferritin proteins were induced by IPTG (1 mM) addition, and cells were incubated for an additional 4 h at 37 °C. After protein induction, cells were collected by

centrifugation, and the pellets were resuspended in 50 mL of a buffer solution containing 50 mM Tris-HCl pH 7.2 and 150 mM NaCl. The solution was sonicated on ice and centrifuged to remove cell debris. The supernatant was treated by 60 °C heat shock, and protein aggregates were removed by centrifugation. The resulting supernatant was finally subjected to size exclusion chromatography (ACTA Pure, GE Healthcare) using a Superose^{TM} 6 10/300 GL column. Protein G-fused ferritin was constructed by introducing a GGGGSGGGGG amino acid linker between antibody binding single domain of protein G[41] and the N-terminus of human ferritin heavy chain. An N-terminal His tag sequence was removed from the pET21a vector to produce intact ferritin proteins. All proteins were stored in 20 mM HEPES pH 7.2 at 4 °C before use.

Preparation of fluorescent Ft-Ag NCs. To prepare the Ft-Ag NCs, 2 μL of $AgNO_3$ solution was added to 200 μL of 200 nM ferritin solution in 20 mM HEPES pH 7.2 to the indicated protein and silver ion ratios. After incubation for 5 min at room temperature, $NaBH_4$ solution was added to the mixture for a 50 μM final concentration. Following additional incubation for 5 min at room temperature with constant mixing, NaCl was added to the solution for a 50 mM final chloride concentration. Following an another 10 min incubation at room temperature, the mixture was centrifuged at 10,000 rpm at 4 °C for 10 min. The supernatant was discarded, and the resulting Ft-Ag NCs were resuspended in 20 mM HEPES pH 7.2. Agarose gel electrophoresis of Ft-Ag NCs and protein G-covered ferritin constructs was performed with 1.5% agarose gels with 0.5X TAE (10 mM acetic acid, 0.5 mM EDTA, and 20 mM Tris pH 8.0) as a running buffer. The agarose gel was analyzed by fluorescence of silver NCs as well as protein staining coomassie blue signals.

Spectroscopic assays. UV-Vis spectra were recorded on a UV Spectrophotometer (Optizen POP Bio), and fluorescence studies of the silver clusters in a sealed cuvette were carried out with a Fluorescence Spectrometer instrument (Perkin Elmer LS55). All fluorescent measurements were carried out with an excitation slit width 5 nm and emission slit width 5 nm. The fluorescence quantum yield of FT-Ag NCs was determined by measuring the integrated fluorescence intensities of the FT-Ag NCs with Rhodamine B in ethanol as the reference standard (QY = 70%).[34] Fluorescence images of silver solutions, electrophoretic gels, and surface hydrogels were obtained with a Bio-Rad imaging system (ChemiDoc^{TM} MP, light source: 470/30 nm blue epi illumination, emission filters: 695/55 nm and 530/28 nm).

Field-emission transmission electron microscopy (FE-TEM). The fabricated silver nanostructures on ferritin proteins were visualized with a FE-TEM (JEM-2100F(HR), JEOL LTD.). Ft-Ag NCs and other reaction solutions were adsorbed onto a carbon-coated copper grid (200 mesh) and air-dried for 2 min. To analyze protein structures, Ft-Ag NCs as well as protein G-fused Ft-Ag NCs were examined with a FE-TEM after negative staining with 2% uranyl acetate (Electron Microscopy Sciences) for 30 sec.

Metal Ion detection. Metal ion solutions (Ca^{2+}, Cd^{2+}, Co^{2+}, Cr^{2+}, Cu^{2+}, Fe^{3+}, Hg^{2+}, Mg^{2+}, Mn^{2+}, Ni^{2+}, and Pb^{2+}) were prepared in Milli-Q water in higher stock concentrations. These solutions were diluted and added to 200 μL of Ft-Ag NCs to 0.1 mM of final metal ion concentrations. The solutions were then incubated at room temperature for 2 min before fluorescence measurements.

Fabrication of hydrogel chips with encapsulated Ft-Ag NCs. A glass slide were soaked in nitric acid solution for 2 h, and washed with acetone. Next, the clean glass slides were treated

with 10% TPM in acetone for 4 h, followed by ethanol washing. After an air dry, the acryl-modified glass slides were stored in a vacuum desiccator before use. 1 μM of Ft-Ag NC or green fluorescent protein (GFP) was added to the acrylamide polymerization solution containing 4% acrylamide monomer (acrylamide:bis-acrylamide = 29:1), 1% photo initiator (2-hydroxy-2-methylpropiophenone), and 30% glycerol Milli-Q water. This mixed solution (4 μL) was spotted on the TPM-modified glass slides by a pipette. After spotting, the slides were placed under UV irradiation for 5 min to trigger the polymerization and form polyacrylamide hydrogels.

Conclusion

In the present study, we assembled water-soluble and fluorescent silver nanoclusters (NCs) on ferritin proteins under a native aqueous buffer condition. Optimized silver reduction on ferritin offered the first example of protein-templated fluorescent silver NCs with retained structures and functions of template proteins including fused binding proteins. We believe that the active metal uptake property of ferritin with an isolated reaction space greatly contributes to homogeneous assembly of fluorescent silver NCs, by allowing precisely controlled silver deposition. The robust and large cage structure of ferritin was utilized to develop a highly stable and porous hydrogel copper-sensing system by simply encapsulating Ft-Ag NCs in low-density hydrogels. More importantly, Ft-Ag NCs can be easily engineered to have diverse functional proteins, as demonstrated with antibody-binding protein G. The present Ft-Ag NCs show great potential as a new fluorescent probe with high structural and functional diversities as well as good biocompatibility and low toxicity. To fully exploit these versatile nanoclusters, however, detailed mechanistic and structural analyses for silver NC assembly on ferritin will follow. In addition, improving the quantum yield of Ft-Ag NCs will

also be highly beneficial for utilization of these functional fluorescent silver NCs in biological sensing and imaging.

Acknowledgements

This research is supported by grants from the National Research Foundation of Korea (NRF 2011-0020322) and Center for BioNano Health-Guard funded by the Ministry of Science, ICT & Future Planning (MSIP) of Korea as Global Frontier Project (H-GUARD_2014M3A6B2060512). J.M.L. is supported by Basic Science Research Program through the National Research Foundation of Korea (NRF 2013R1A1A2064140).

Note and references

[a] *Department of Chemistry, Korea Advanced Institute of Science and Technology, Daejeon 305-701, Korea. E-mail: ywjung@kaist.ac.kr*

[b] *BioNanotechnology Research Center, Korea Research Institute of Bioscience and Biotechnology, P.O. Box 115, Daejeon 305-600, Korea*

† Electronic Supplementary Information (ESI) available, See DOI: 10.1039/b000000x/

1 J. Zheng, P. R. Nicovich and R. M. Dickson, *Annu. Rev. Phys. Chem.*, 2007, **58**, 409-431.

2 C. J. Lin, C. H. Lee, J. T. Hsieh, H. H. Wang, J. K. Li, J. L. Shen, W. H. Chan, H. I. Yeh and W. H. Chang, *J. Med. Biol. Eng.*, 2009, **29**, 276-283.

3 H. Hakkinen, *Chem. Soc. Rev.*, 2008, **37**, 1847-1859.

4 L. Shanga, S. Dong and U. Nienhaus, *Nano Today*, 2011, **6**, 401-418.

5 Y. Lu and W. Chen, *Chem. Soc. Rev.*, 2012, **41**, 3294-3623.

6 H. Xu and K. S. Suslick, *Adv. Mater.*, 2010, **22**, 1078-1082.

7 T. Linnert, P. Mulvaney, A. Henglein and H. WeUer, *J. Am. Chem. Soc.*, 1990, **112**, 4657-4664.

8 T. Vosch, Y. Antoku, J. C. Hsiang, C. I. Richards, J. I. Gonzalez and R. M. Dickson, *Proc. Natl. Acad. Sci. U. S. A.*, 2007, **104**, 12616-12621.

9 J. T. Petty, J. Zheng, N. V. Hud and R. M. Dickson, *J. Am. Chem. Soc.*, 2004, **126**, 5207-5212.

10 C. I. Richards, S. Choi, J. C. Hsiang, Y. Antoku, T. Vosch, A. Bongiorno, Y. L. Tzeng and R. M. Dickson, *J. Am. Chem. Soc.*, 2008, **130**, 5038-5039.

11 A. Latorre and Á. Somoza, *Chembiochem*, 2012, **13**, 951-958.

12 J. M. Obliosca, C. Liu, R. A. Batson, M. C. Babin, J. H. Werner and H. C. Yeh, *Biosensors*, 2013, **3**, 185-200.

13 J. M. Obliosca, C. Liu and H. C. Yeh, *Nanoscale*, 2013, **5**, 8443-8461.

14 C. Guo and J. Irudayaraj, *Anal. Chem.*, 2011, **83**, 2883-2889.

15 S. Ghosh, U. Anand and S. Mukherjee, *Anal. Chem.*, 2014, **86**, 3188-3194.

16 B. Li, J. Li and J. Zhao, *Spectrochim Acta A Mol. Biomol. Spectrosc.*, 2015, **134**, 40-47.

17 T. Zhou, Y. Huang, W. Li, Z. Cai, F. Luo, C. J. Yang and X. Chen, *Nanoscale*, 2012, **4**, 5312-5315.

18 S. S. Narayanan and S. K. Pal, *J. Phys. Chem. C*, 2008, **112**, 4874-4879.

19 M. Uchida, S. Kang, C. Reichhardt, K. Harlen and T. Douglas, *Biochim. Biophys. Acta*, 2010, **1800**, 834-845.

20 P. M. Harrison and P. Arosio, *Biochim. Biophys. Acta Bioenerg.*, 1996, **1275**, 161-203.

21 R. M. Kramer, C. Li, D. C. Carter, M. O. Stone and R. R. Naik, *J. Am. Chem. Soc.*, 2004, **126**, 13282-13286.

22 T. Todd, Z. Zhen and J. Xie, *Nanomedicine*, 2013, **8**, 1555-1557.

23 C. Sun, H. Yang, Y. Yuan, X. Tian, L. Wang, Y. Guo, L. Xu, J. Lei, N. Gao, G. J. Anderson, X. J. Liang, C. Chen, Y. Zhao and G. Nie, *J. Am. Chem. Soc.*, 2011, **133**, 8617-8624.

24 C. A. Butts, J. Swift, S. G. Kang, L. D. Costanzo, D. W. Christianson, J. G. Saven and I. J. Dmochowski, *Biochemistry*, 2008, **47**, 12729-12739.

25 O. Kasyutich, A. Ilari, A. Fiorillo, D. Tatchev, A. Hoell and P. Ceci, *J. Am. Chem. Soc.*, 2010, **132**, 3621-3627.

26 J. M. Domínguez-Vera, N. Gálvez, P. Sánchez, A. J. Mota, S. Trasobares, J. C. Hernández and J. J. Calvino, *Eur. J. Inorg. Chem.*, 2007, **30**, 4823-4826.

27 G. Y. Lan, C. C. Huang and H. T. Chang, *Chem. Commun.*, 2010, **46**, 1257-1259.

28 L. Shanga and S. Dong, *J. Mater. Chem.*, 2008, **18**, 4636-4640.

29 Z. M. and B. C. Ye, *Analyst*, 2011, **136**, 5139-5142.

30 Y. Zhou, T. Zhou, M. Zhang and G. Shi, *Analyst*, 2014, **139**, 3122-3126.

31 G. Liu, D. Q. Feng, T. Chen, D. Li and W. Zheng, *J. Mater. Chem.*, 2012, **22**, 20885-20888.

32 B. Han and E. Wang, *Biosens. Bioelectron.*, 2011, **26**, 2585-2589.

33 W. Y. Chen, G. Y. Lan and C. H. T., *Anal. Chem.*, 2011, **83**, 9450-9455.

34 F. L. Arbeloa, P. R. Ojeda and I. L. Arbeloa, *J. Luminesc.*, 1989, **44**, 105-112.

35 A. S. Patel and T. Mohanty, *J. Mater. Sci.*, 2014, **49**, 2136-2143.

36 S. Roy, A. Baral and A. Banerjee, *ACS Appl. Mater. Interfaces*, 2014, **6**, 4050-4056.

37 A. Baksi, M. S. Bootharaju, X. Chen, H. Hakkinen and T. Pradeep, *J. Phys. Chem. C*, 2014, **118**, 21722-21729.

38 S. Roy and A. Banerjee, *Soft Matter*, 2011, **7**, 5300-5308.

39 B. Adhikari and A. Banerjee, *Chem. Eur. J.*, 2010, **16**, 13698-13705.

40 B. Adhikari and A. Banerjee, *Chem. Mater.*, 2010, **22**, 4364-4371.

41 Y. Jung, J. Y. Jeong and B. H. Chung, *Analyst*, 2008, **133**, 697-701.

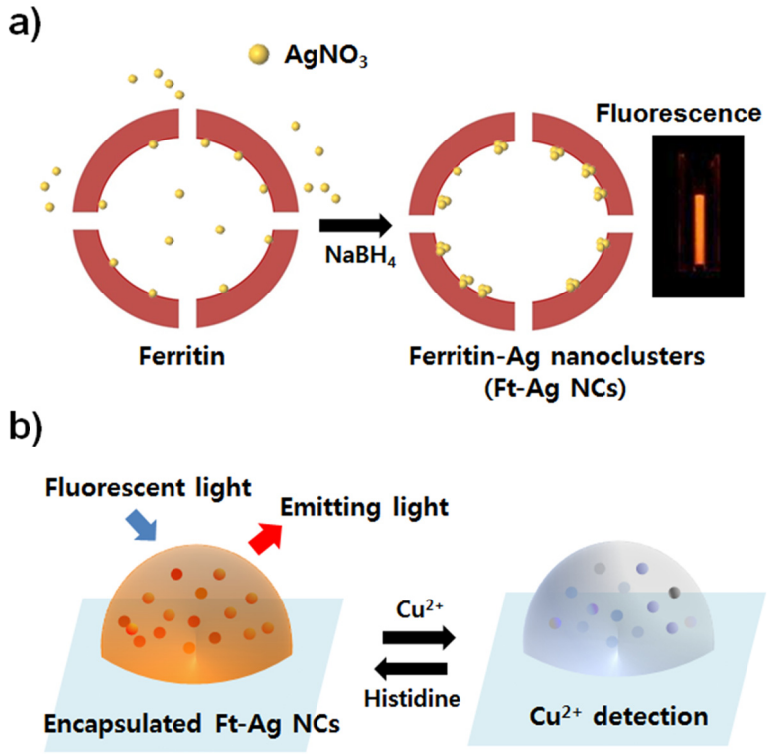

Fig. 1 Schematic representations of (a) the synthesis of ferritin-templated fluorescent silver NCs (Ft-Ag NCs) and (b) a Ft-Ag NCs-embedded hydrogel sensor.

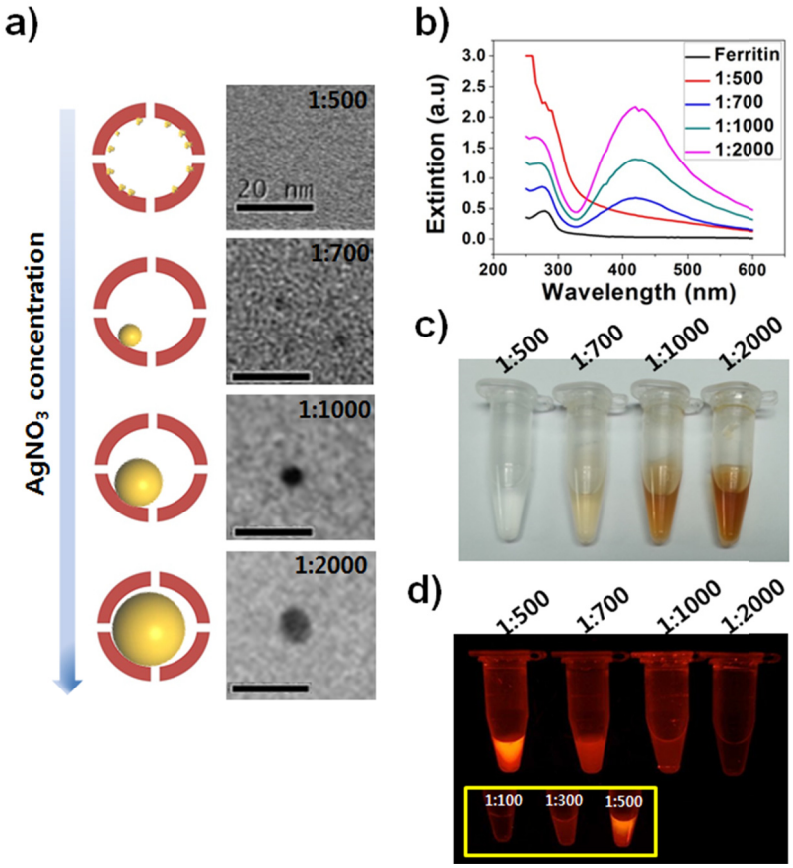

Fig. 2 Ferritin-templated synthesis of silver nanostructures. (a) Representative TEM images of silver nanostructures formed on ferritin in various protein/$AgNO_3$ ratios. Scale bars, 20 nm. (b) UV-Vis spectra of free ferritin protein and ferritin-templated silver nanostructures. (c) Color analysis of ferritin-templated silver nanostructures. (d) Fluorescence images of ferritin-templated silver nanostructures. The ferritin/$AgNO_3$ ratios are indicated.

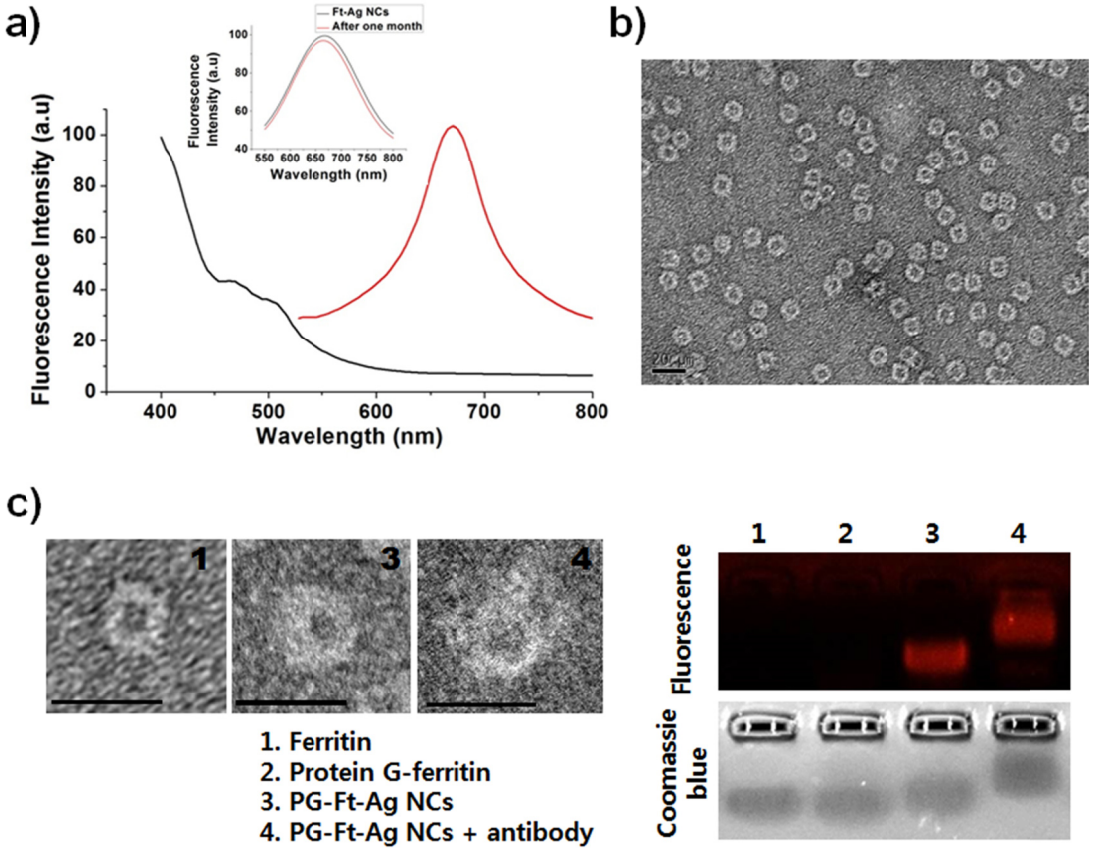

Fig. 3 Characterization of Ft-Ag NCs. (a) Fluorescence excitation (black) and emission (red) spectra of Ft-Ag NCs. The inset shows maintained fluorescence properties of purified Ft-Ag NCs after one month. (b) A TEM image of purified Ft-Ag NCs. Scale bar, 20 nm. (c) TEM (left) and 1.5% agarose gel (right) analyses of (1) free ferritin protein, (2) protein G-fused ferritin (PG-Ft), (3) PG-Ft templated silver NCs (PG-Ft-Ag NCs), and (4) PG-Ft-Ag NCs incubated with an antibody. The agarose gel was analyzed by fluorescence (top) as well as protein staining coomassie blue signals (bottom). Scale bar, 20 nm.

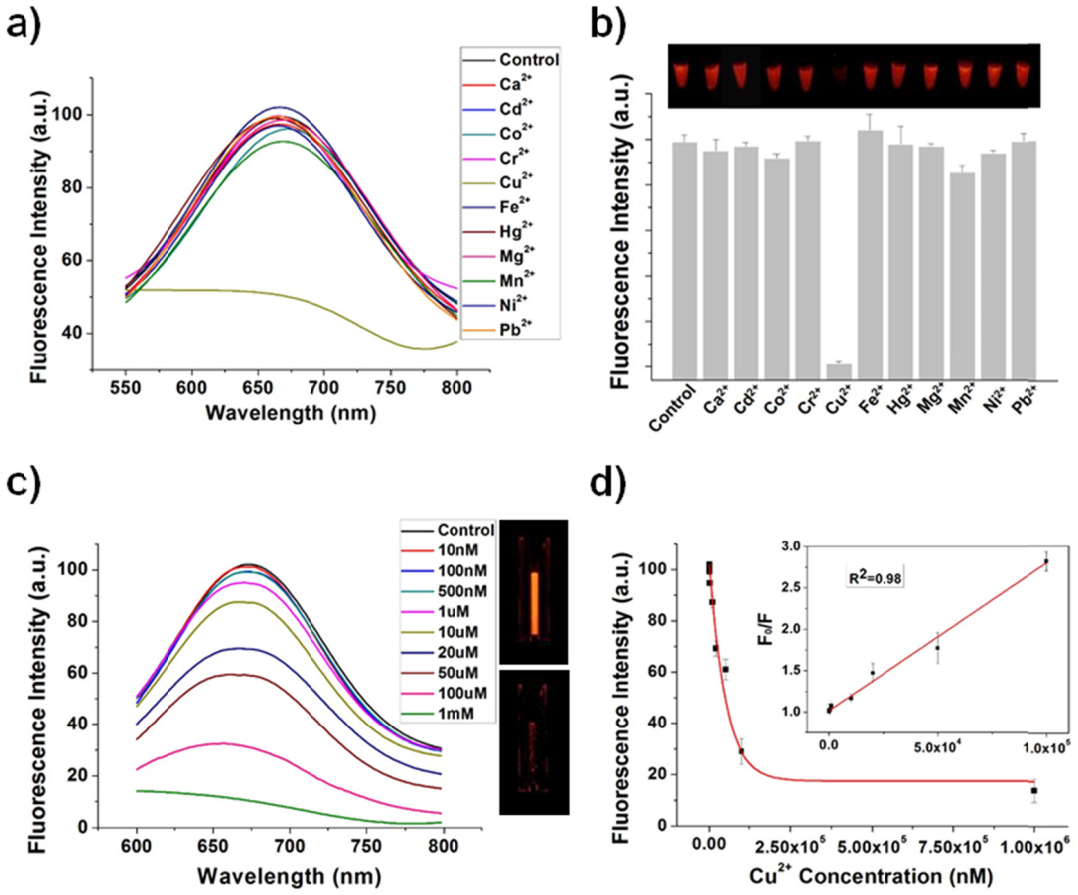

Fig. 4 Cu^{2+}-specific fluorescence quenching of Ft-Ag NCs. (a) Fluorescence emission spectra of Ft-Ag NCs after incubation with various metal ions. (b) Relative degrees of quenching of Ft-Ag NCs by various metal ions. (c) Fluorescence emission spectra of Ft-Ag NCs after incubation with varying concentrations of Cu^{2+}. (d) Quantitative representation of fluorescence quenching by varying concentrations of Cu^{2+}. The inset is the Stern-Volmer plot of fluorescent quenching. The error bars correspond to the standard error of the mean of three independent measurements.

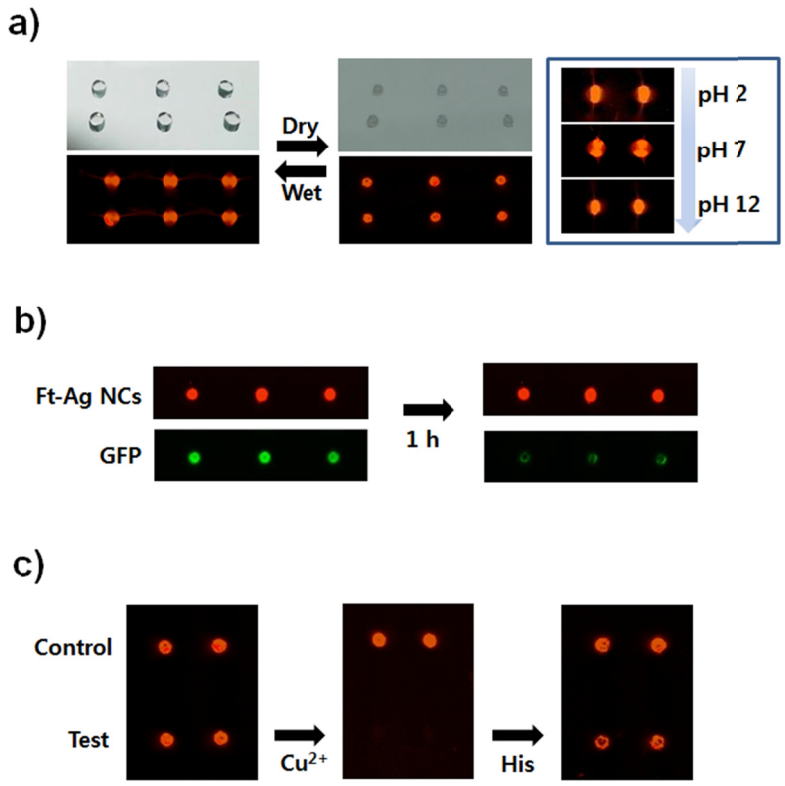

Fig. 5 Fluorescence images of Ft-Ag NC-encapsulated hydrogel sensor chips. (a) A glass chip with Ft-Ag NC encapsulated hydrogel spots and its fluorescence images. Hydrogel spots and fluorescence signals were imaged in dried and subsequently hydrated conditions. The right inset shows fluorescence images of Ft-Ag NC-encapsulated hydrogels in varying pH solutions from pH 2 to 12, (b) Fluorescence images of Ft-Ag NC (top) or GFP (bottom) embedded hydrogels during 1 h incubation in a aqueous buffer solution. (c) Fluorescence images of Ft-Ag NC-encapsulated hydrogels upon Cu^{2+} and subsequent histidine treatment.